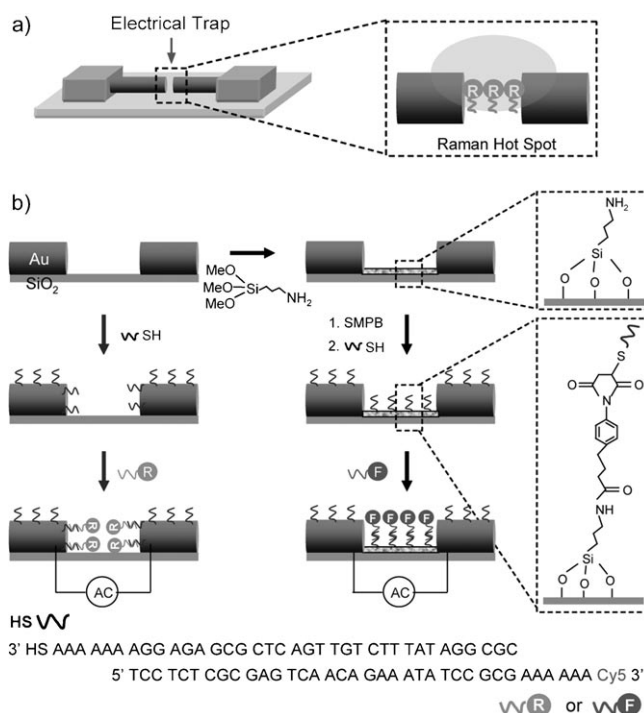


## Spectroscopically Enhancing Electrical Nanotraps\*\*

Gengfeng Zheng, Lidong Qin, and Chad A. Mirkin\*

One of the greatest challenges in nanoscience is the development of efficient methods for physically probing or trapping a nanomaterial or small collection of molecules<sup>[1]</sup> with the capability to spectroscopically identify these entities. The small size of nanomaterials often prohibits the use of conventional spectroscopic tools to locate and identify them. Scanning-probe technologies allow nanomaterials to be physically placed and characterized on a surface,<sup>[2–4]</sup> and single-molecule spectroscopies allow individual molecules or particles to be observed,<sup>[5,6]</sup> but only if they can be addressed; to do so, relatively high concentrations of the probe molecules (ca. 100 pM) are typically required.<sup>[7]</sup> A method for rapidly concentrating a nanomaterial or set of molecules to be probed in a nanoscale reaction vessel coupled with the ability to spectroscopically identify such materials would be a significant advance. Herein, we show how nanogap structures, prepared by on-wire lithography (OWL),<sup>[8,9]</sup> can be used to localize biomolecules with an electric field and provide a powerful means to spectroscopically identify them based upon surface-enhanced Raman spectroscopy (SERS).<sup>[9–11]</sup>

Recently, we developed the OWL method for fabricating one-dimensional wire structures with precise control over the compositional blocks that comprise such wires and the ability to modulate gap size by OWL, especially in the context of gold or silver wire components, allows enhancing “hot-spots” for Raman spectroscopy to be created. Indeed, the level of Raman enhancement of such structures can be tuned by controlling the gap dimensions and separation distance.<sup>[9]</sup> We hypothesized that we could use the OWL process to create gold electrodes separated by a nanoscale distance that would optimize SERS activity in the gap and, perhaps, allow an alternating (AC) electric field to drive charged entities into the gap where the strongest electric field gradient exists (Scheme 1 a).<sup>[12]</sup> With microscale electrodes, electric fields can be used to enhance hybridization in the context of DNA detection.<sup>[12–14]</sup> In this way, we could physically trap a nanoscopic amount of material at a low concentration in solution and gain the ability to spectroscopically identify it under highly enhancing conditions.



**Scheme 1.** a) An OWL-gap electrical device, with the trapped target molecules in the Raman hot spots. b) Schematic view of surface functionalization of OWL gaps and hybridization with DNA targets. Alkanethiol-terminated oligonucleotides (the receptor strand) can be directly linked to the gold segments that form the gap (left), or coupled to the silica within the gap, which was premodified with 3-aminopropyl trimethoxysilane and then succinimidyl-4-(*p*-maleimidophenyl)butyrate (SMPB) (right). The target oligonucleotides modified with Raman (R, left) or fluorescence dyes (F, right) are trapped inside the gaps when an AC electric field is applied. The oligonucleotide sequences used in this paper are shown at the bottom of the scheme.

The fabrication of the electrical nanotraps includes three key steps: the synthesis of Raman-optimized nanogaps by the OWL method,<sup>[8,9,15]</sup> fabrication of metal microelectrodes by conventional lithographic techniques, and surface functionalization of the nanogaps with the appropriate molecules (e.g. oligonucleotides or other receptors for the analytes of interest).<sup>[16]</sup> Alkanethiol-terminated oligonucleotides can be directly linked to gold portions of the gap, or coupled to the silica within the gap that has been premodified with 3-aminopropyl trimethoxysilane and succinimidyl-4-(*p*-maleimidophenyl)butyrate (SMPB) (Scheme 1 b and Supporting Information). Proof-of-concept electrical trap structures consisting of gold–gap–gold architectures (3, 1.5, and 3 μm, respectively, Figure 1 a,b) fabricated by OWL and functionalized with DNA were initially characterized by fluorescence microscopy. These structures were rinsed with phosphate

[\*] G. Zheng, L. Qin, Prof. C. A. Mirkin  
Department of Chemistry and  
International Institute for Nanotechnology  
Northwestern University  
2145 Sheridan Road, Evanston, IL 60208-3113 (USA)  
Fax: (+1) 847-467-5123  
E-mail: chadnano@northwestern.edu

[\*\*] C.A.M. acknowledges the AFOSR, DARPA, ONR, and NSF for the support of this research. C.A.M. is also grateful for the NIH Director's Pioneer Award.

Supporting information for this article is available on the WWW under <http://www.angewandte.org> or from the author.

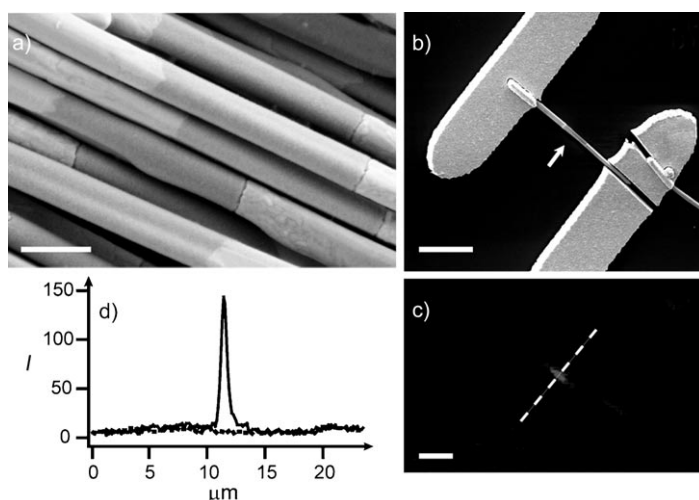


**Figure 1.** a) An SEM image of as-synthesized nanorods. The darker central nickel portion will be etched away to form gap structures. b) SEM image and c) corresponding fluorescence image of a representative microgap device showing the localization of Cy5-labeled DNA in the gap. The gap position is indicated by the white arrow. d) Line profile of the fluorescence intensity (solid line), corresponding to the white broken line in c), and fluorescence line profile of a gap without an applied field (dotted line). Scale bars in (a), (b), and (c) are 500 nm, 2 μm, and 2 μm, respectively.

buffer, and then interfaced with the prefabricated microelectrodes (see Supporting Information). A phosphate buffer solution containing 1 nM Cy5-labeled oligonucleotide which is complementary to the DNA functionalized in the gap and 20 mM NaCl was flowed over the immobilized traps by a microfluidic channel (volume = 1 μL). The salt concentration is deliberately low, as the electric field can cover a larger distance under conditions where it is less screened.<sup>[17]</sup> In addition, under these conditions, the amount of DNA target binding outside of the active gap area is significantly reduced. Indeed, lower salt concentration and decreased oligonucleotide concentration favor the unhybridized state. Scanning electron microscopy (SEM) and fluorescence images of the trap device under potential control ( $V_{p-p} = 0.8\text{--}1.2$  V,  $f = 1\text{--}10$  kHz) clearly show that the fluorophore-labeled oligonucleotide is concentrated in the gap region (Figure 1 b,c). In a control experiment, gaps on the same chip without an applied field show no detectable fluorescence under identical conditions. Line profiles of fluorescence intensity across the gap under potential control show an increase in fluorescence by a factor of 20 as compared to the control experiment with no applied field (Figure 1 d).

The demonstration of analyte localization under an applied field in a microtrap structure is well known.<sup>[12–14]</sup> However, if nanotrap structures are fabricated with materials that have surface plasmon resonances, the gap size can be optimized so that materials localized within the gap are detectable by SERS.<sup>[9]</sup> SERS is a phenomenon that was discovered 30 years ago and has been studied in the context of many types of nanostructured interfaces.<sup>[11,18]</sup> In principle, with nanoscale gaps SERS could be used in conjunction with applied electric fields to locally concentrate, address, and

spectroscopically identify charged materials. To evaluate the potential of nanotraps for simultaneous analyte recognition and spectroscopic identification, we used OWL to fabricate sub-100-nm gap structures with gold segments on the opposite sides of the nanogaps. As such structures have been shown to act as Raman “hot spots” with enhancement factors as large as  $10^8$ ,<sup>[9]</sup> target molecules electrically driven into them can be efficiently identified by SERS. In a typical experiment, a nanotrap device with a 50-nm gap (Figure 2 a,b) was used to electrically localize DNA target molecules using an AC field as described for the aforementioned microgap architectures, and the Raman spectra and images of the gap area were measured by a confocal scanning Raman

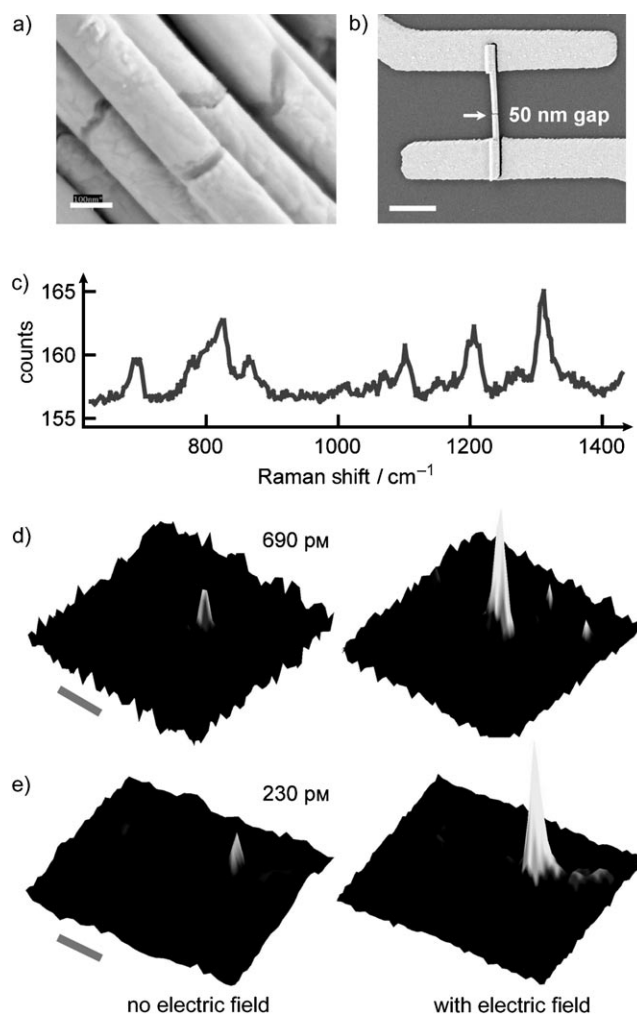


**Figure 2.** a) An SEM image of the as-synthesized OWL nanorods. The darker central nickel portion will be etched away to form gap structures. b) An SEM image of a nanogap device contacting with electrodes. Gap size is 50 nm. c) Raman spectrum of the Cy5-labeled DNA target between 650 and 1450 cm<sup>-1</sup>. The Raman intensity of each pixel in (d) and (e) was determined by integrating over this spectral region. d,e) Scanning Raman microscopy images showing that Raman intensities significantly increased owing to the accumulation of target DNA (at concentrations indicated) by an electric field into the nanogaps that function as Raman hot spots. Scale bars in (a), (b), (d), and (e) are 200 nm, 2 μm, 1 μm, and 1 μm, respectively.

microscope (see Supporting Information). For evaluation of the magnitude of the electrical trapping effect, nanogap devices were first characterized by hybridizing Cy5-linked DNA targets in the absence of an electric field. These structures were then completely dehybridized by immersing them into deionized water at 80°C (as evidenced by a complete loss of Raman signal) and then used to capture the same DNA with an applied AC field. The Raman signal was measured in a cyclical fashion after each hybridization and dehybridization step in the absence and presence of an applied electric field. A comparison of the three-dimensional scanning Raman microscopy images of two nanogap devices, both with and without an applied electric field, clearly show that the field effectively localizes and increases the amount of DNA that enters and gets trapped in the device structure (Figure 2d,e). It is clear that when the electric field was applied for target trapping, the center of the nanogaps exhibit an intense Raman signal, which appears as a bright band against a dark, smooth background. Little Raman signal is observed from the flat portions of the nanotrap and chip surface,<sup>[9,19]</sup> as both the concentration of bound targets and the efficiency of Raman enhancement in these areas are much lower than inside the nanogaps. For the two concentrations of DNA targets studied (690 and 230 pM), the Raman intensity increased 40 and 20 times in total integration of the peak area as a result of applied field, respectively. These experiments demonstrate that under this electrode configuration, SERS can be used to obtain spectroscopic information about the molecules driven into a nanogap by an applied electric field.

These nanotraps can be used to detect DNA in a moderately sensitive manner (Figure 3a,b). In our proof-of-concept experiments, the lowest measurable DNA concentration is 230 fM, which is over 20 times more sensitive than

previous nanogap Raman detection results without an applied field (i.e. 5 pM),<sup>[19]</sup> and at least twice the sensitivity of reported methods based upon tip-enhanced-Raman spectroscopy (TERS).<sup>[4]</sup> If taken into account that the OWL approach allows such structures to be routinely fabricated and interface them with conventional circuitry, the approach is more attractive than TERS and near-field scanning optical microscopy techniques that require complicated experimental instrumentation.<sup>[3,4]</sup> Moreover, our experiments demonstrate how microfluidic devices can be coupled with the nanotraps to effectively deliver and concentrate target from 1  $\mu$ L samples, making the structures excellent candidates for lab-on-chip applications. In principle, the new OWL-based nanotrap method can be further improved by optimizing the electric field parameters,<sup>[12]</sup> designing different nanogap structures/materials, or using nanoparticle-functionalized DNA probes for signal magnification.<sup>[20]</sup> Indeed, this approach, which combines the relatively high throughput OWL fabrication approach, the concept of Raman hot spots, and high efficiency electric field trapping, may open up a host of new opportunities for integrating SERS nanostructures and lab-on-chip electrical nanodevices<sup>[21]</sup> for many applications in the life sciences.<sup>[22]</sup>

Received: November 19, 2007

Published online: January 28, 2008

**Keywords:** DNA · electric field · lithography · nanotechnology · surface-enhanced Raman spectroscopy

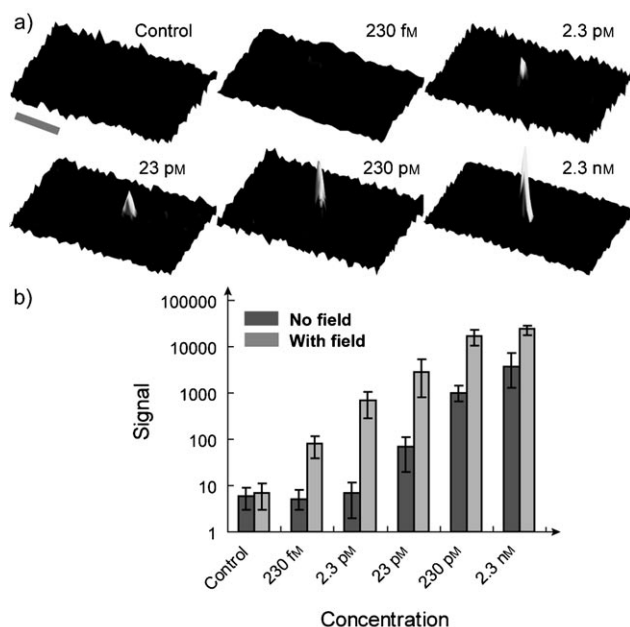


**Figure 3.** a) Scanning Raman microscopy images of nanotraps under an applied electric field in the context of DNA detection. The scale bar is 1  $\mu$ m. b) Raman intensity as a function of target concentration with (dark bars) and without (light gray bars) an applied electric field.

- [1] R. Hölzel, N. Calander, Z. Chiragwandi, M. Willander, F. F. Bier, *Phys. Rev. Lett.* **2005**, 95, 128102.
- [2] a) R. D. Piner, J. Zhu, F. Xu, S. H. Hong, C. A. Mirkin, *Science* **1999**, 283, 661–663; b) K. Salaita, Y. Wang, C. A. Mirkin, *Nat. Nanotechnol.* **2007**, 2, 145–155; c) C. A. Mirkin, *ACS Nano* **2007**, 1, 79–83.
- [3] a) E. Betzig, R. J. Chichester, *Science* **1993**, 262, 1422–1425; b) J. K. Gimzewski, C. Joachim, *Science* **1999**, 283, 1683–1688.
- [4] a) J. A. Dieringer, A. D. McFarland, N. C. Shah, D. A. Stuart, A. V. Whitney, C. Y. Yonzon, M. A. Young, X. Zhang, R. P. Van Duyne, *Faraday Discuss.* **2006**, 132, 9–26; b) B. Pettinger, G. Picardi, R. Schuster, G. Ertl, *Single Mol.* **2002**, 3, 285–294.
- [5] a) S. Weiss, *Science* **1999**, 283, 1676–1683; b) X. Michalet, S. Weiss, M. Jäger, *Chem. Rev.* **2006**, 106, 1785–1813.
- [6] a) B. C. Stipe, M. A. Rezaei, W. Ho, *Science* **1998**, 280, 1732–1735; b) L. Yu, Z. K. Keane, J. W. Ciszek, L. Cheng, M. P. Stewart, J. M. Tour, D. Natelson, *Phys. Rev. Lett.* **2004**, 93, 266802; c) W. Liang, M. P. Shores, M. Bockrath, J. R. Long, H. Park, *Nature* **2002**, 417, 725–729.
- [7] a) H. P. Lu, L. Xun, X. S. Xie, *Science* **1998**, 282, 1877–1882; b) E. A. Lipman, B. Schuler, O. Bakajin, W. A. Eaton, *Science* **2003**, 301, 1233–1235; c) M. P. Gordon, T. Ha, P. R. Selvin, *Proc. Natl. Acad. Sci. USA* **2004**, 101, 6462–6465.
- [8] a) L. Qin, S. Park, L. Huang, C. A. Mirkin, *Science* **2005**, 309, 113–115; b) L. Qin, M. J. Banholzer, X. Xu, L. Huang, C. A. Mirkin, *J. Am. Chem. Soc.* **2007**, 129, 14870–14871.
- [9] L. Qin, S. Zou, C. Xue, A. Atkinson, G. C. Schatz, C. A. Mirkin, *Proc. Natl. Acad. Sci. USA* **2006**, 103, 13300–13303.
- [10] S. M. Nie, S. R. Emery, *Science* **1997**, 275, 1102–1106.
- [11] a) C. L. Haynes, A. D. McFarland, R. P. Van Duyne, *Anal. Chem.* **2005**, 77, 338A–346A; b) H. Wang, C. S. Levin, N. J. Halas, *J. Am. Chem. Soc.* **2005**, 127, 14992–14993.

- [12] a) N. G. Green, A. Ramos, A. Gonzalez, H. Morgan, A. Castellanos, *Phys. Rev. E* **2000**, *61*, 4011–4018; b) K. F. Hoettges, M. McDonnell, M. P. Hughes, *J. Phys. D* **2003**, *36*, L101–L104; c) P. K. Wong, C. Y. Chen, T. H. Wang, C. M. Ho, *Anal. Chem.* **2004**, *76*, 6908–6914; d) R. J. Barsotti, M. D. Vahey, R. Wartena, Y. M. Chiang, J. Voldman, F. Stellacci, *Small* **2007**, *3*, 488–499.
- [13] C. F. Chou, T. O. Tegenfeldt, O. Bakajin, S. S. Chan, E. C. Cox, N. Darnton, T. Duke, R. H. Austin, *Biophys. J.* **2002**, *83*, 2170–2179.
- [14] a) C. F. Edman, D. E. Raymond, D. J. Wu, E. G. Tu, R. G. Sosnowski, W. F. Butler, M. Nerenberg, M. J. Heller, *Nucleic Acids Res.* **1997**, *25*, 4907–4914; b) C. Gurtner, E. Tu, N. Jamshidi, R. W. Haigis, T. J. Onofrey, C. F. Edman, R. Sosnowski, B. Wallace, M. J. Heller, *Electrophoresis* **2002**, *23*, 1543–1550.
- [15] a) C. R. Martin, *Science* **1994**, *266*, 1961–1966; b) B. R. Martin, D. J. Dermody, B. D. Reiss, M. M. Fang, L. A. Lyon, M. J. Natan, T. E. Mallouk, *Adv. Mater.* **1999**, *11*, 1021–1025; c) S. R. Nicewarner-Pena, R. G. Freeman, B. D. Reiss, L. He, D. J. Pena, I. D. Walton, R. Cromer, C. D. Keating, M. J. Natan, *Science* **2001**, *294*, 137–141.
- [16] a) S. I. Stoeva, J. S. Lee, J. E. Smith, S. T. Rosen, C. A. Mirkin, *J. Am. Chem. Soc.* **2006**, *128*, 8378–8379; b) G. Zheng, F. Patolsky, Y. Cui, W. U. Wang, C. M. Lieber, *Nat. Biotechnol.* **2005**, *23*, 1294–1301.
- [17] K. H. Bhatt, S. Grego, O. D. Velev, *Langmuir* **2005**, *21*, 6603–6612.
- [18] a) K. Kneipp, Y. Wang, H. Kneipp, L. T. Perelman, I. Itzkan, R. , Dasari, M. S. Feld, *Phys. Rev. Lett.* **1997**, *78*, 1667–1670; b) A. Tao, F. Kim, C. Hess, J. Goldberger, R. He, Y. Sun, Y. Xia, P. Yang, *Nano Lett.* **2003**, *3*, 1229–1233.
- [19] L. Qin, M. J. Banholzer, J. E. Millstone, C. A. Mirkin, *Nano Lett.* **2007**, *7*, 3849–3853.
- [20] N. L. Rosi, C. A. Mirkin, *Chem. Rev.* **2005**, *105*, 1547–1562.
- [21] a) H. Craighead, *Nature* **2006**, *442*, 387–393; b) C. D. Chin, V. Linder, S. K. Sia, *Lab Chip* **2007**, *7*, 41–57.
- [22] a) M. C. Roco, *Curr. Opin. Biotechnol.* **2003**, *14*, 337–346; b) M. Ferrari, *Nat. Rev. Cancer* **2005**, *5*, 161–171.